

Wavelet Spectrum Extracted from Coastal Marine Radar Images

Dong Jiing DOONG Li Chung WU Chia Chuen KAO Laurence Zsu Hsin CHUANG

Department of Hydraulic and Ocean Engineering,
National Cheng Kung University
Tainan, Taiwan, ROC

Coastal Ocean Monitoring Center,
National Cheng Kung University
Tainan, Taiwan, ROC

ABSTRACT

Ocean waves are extremely random and are directly and indirectly dependent on meteorological, hydrological, oceanographic and topographical factors. Field measurements must be performed to increase the knowledge of ocean waves. Remote sensing techniques have become quite popular for ocean wave measurement applications. Microwave RADAR that can provide all weather monitoring during day and night and is less affected by cloud and rain is now the most popular sensor of remote sensing techniques among others. The spectrum represents the distribution of wave energy. The wave parameters such as wave height, period, direction and wavelength are derived from wave spectrum. It is therefore important to derive the spectral information from remote sensing images. However, the nearshore images feature non-homogeneity. It is therefore the purpose of this study to develop a non-homogeneous image spectrum analysis method in order to extract the spectral information. This method is developed based on two-dimensional Wavelet transform which has space–frequency representation. The derived image spectrum is called the Wavelet Spectrum. This paper presents the derivation and validation of this method.

KEY WORDS: Remote sensing; non-homogeneous; Wavelet transform

INTRODUCTION

Ocean wave information is required for various purposes, such as coastal engineering, environment protection, port operations, disaster prevention and rescue. Wave data are obtained from many methods, such as theoretic analysis, laboratory experiment, numerical simulation and field measurement. Because the ocean waves, which feature extremely random, are directly and indirectly dependent to meteorological, hydrological, oceanographic and topographical factors,

they cannot be fully understood only by theoretical or numerical approaches. Field measurement must be performed to increase the knowledge of waves. Diverse ways of wave measurement have been investigated since last few decades. They may be categorized as in-situ measurements and remote sensing techniques. At present, various in-situ measurements have significantly developed and improved to better quality, however it is not easy to collect space information. The remote sensing technique has good capability to observe large space ocean wave information. Remote sensing images present the spatial pattern by reflected microwave echoes after a series of electromagnetic pulses is transmitted towards the ocean. During the electromagnetic energy travels from its source to the target, it will come in contact with and interact with the atmosphere it pass through. The receive sensor is required to collect and process the signal which is scattered from the target. Furthermore, since the variation of water surface presented in the images only with the intensity of backscatter showed as the gray levels, it's not allowed to estimate the wave height directly from the images in terms of quantity. Remote sensing images record the distribution of back scattering strength of radar echoes from sea surface. The wave spectrum represents the distribution of wave energy. The wave parameters such as wave height, period, direction and wavelength are derived from wave spectrum. It is therefore important to derive the spectral information from remote sensing images. The derivation of spectral information from remote sensing images does not directly yield the wave spectrum, the relationship between wave spectrum and spectral information from remote sensing images can be described by modulation transfer function.

The Fourier transform is always used to convert the image data into spectrum. For example, Kuo et al. (1999) used the two-dimensional FFT to investigate the image spectrum and calculate the wave parameters from Synthetic Aperture Radar (SAR) images of ERS-1 satellite. Borge et al. (1999) applied the three-dimensional FFT to derive the wave information from nautical radar images. However, some remote sensing images fail to derive the image spectrum by Fourier transform,

especially when the images locate in the nearshore waters (Doong et al., 2001). One of the reasons is the non-homogeneity property in the nearshore image. Therefore, applying the non-homogeneous image spectrum analysis method is one of the solutions. Many methods have been developed in the past few decades, such as the Short-time Fourier transform (Bendat and Piersol, 1986) and more recently, the Wavelet transform (Daubechies, 1990). The Wavelet transform allows exceptional localization in the space domain via translations of the so-called mother wavelet, and in the frequency domain via dilations (Kaiser, 1994). It is recognized as a powerful tool for non-homogeneous signal analysis.

Although Wavelet analysis is recognized as a fruitful technique in signal and image process, the application of Wavelet analysis to ocean engineering or oceanography is still not frequent. Massel (2001) summarized several transform theories and demonstrated Wavelet transform's capabilities in time-frequency representation of Wavelet transform by testing several wave signals. In this study, the Wavelet transform is extended to two-dimensional in order to execute the image spectrum analysis. The performance of the derived non-homogeneous image spectrum analysis method is tested by analyzing simulated homogeneous and non-homogeneous images. Then it is applied to extract the image spectrum from the field marine radar images for applications.

NON-HOMOGENEOUS IMAGE SPECTRUM ANALYSIS METHOD

The Fourier Transform (FT) is used when one is interested in what spectral components exist in the signal. If one wants to know what spectral component occurs at what time, the Fourier transform is not a good choice. The solution to insert time information into the frequency domain of the signal is to divide the signal into segments small enough so that the signal can be assumed stationary. For each segment, the Fourier transform is applied. This approach is known as the Short-time Fourier Transform (STFT). When the window width is assumed as infinite, like the Fourier transform, a good frequency resolution is found. However, the time resolution is lost. When the window width is finite, like the STFT, the frequency resolution is thus not perfect. Therefore, the window width is a key point. The Wavelet transform, described in the following section, has the balance of time/space–frequency resolutions, is used for spectral analysis in this study.

Two-Dimensional Wavelet Transform (2D WT)

The Wavelet transform (WT) is similar to the Fourier transform in that it breaks a signal down into its constituents. Whist the FT breaks the signal into a series of sine waves of different frequencies, WT breaks the signal into *wavelets* which are scaled and shifted versions of the so called *mother wavelet*. WT allows exceptional localization both in the time domain via translations of the wavelet, and in the frequency domain via dilations. The time/space – frequency resolution scheme is shown in Fig. 1. In the one-dimensional wavelet analysis, the signal is multiplied with the wavelet, and the transform is separately computed for different segments of the time domain signal. For the image proceeding in this study, the focus is on the Wavelet transform in two dimensions. The 2D

WT is a very efficient and flexible tool in image analysis, that is, for the detection and measurement of certain characteristic features in images (Cloute et al., 1995). The 2D WT is characterized by a rotation parameter, in addition to the usual translations and dilations. The 2D Wavelet transform is the inner product of $g(\bar{x})$ with a wavelet mother function, is defined as the following:

$$S(a, \bar{b}, \mathbf{q}) = \frac{1}{a} \int_{-\infty}^{\infty} \int_{-\infty}^{\infty} g(x, y) \cdot \bar{\mathcal{Y}}_{a, \bar{b}, \mathbf{q}}(x, y) dx dy \quad (1)$$

where

$$\mathcal{Y}_{a, \bar{b}, \mathbf{q}}(\bar{x}) = \frac{1}{a} \cdot \mathcal{Y} \left[\frac{r_{-\mathbf{q}}(\bar{x} - \bar{b})}{a} \right] \quad (2)$$

The $\mathcal{Y}_{a, \bar{b}, \mathbf{q}}(x, y)$ is the wavelet function which is considered as a function of dilation, displacement and rotation of mother function $\mathcal{Y}(x, y)$ as Eq. (2). $\bar{\mathcal{Y}}_{a, \bar{b}, \mathbf{q}}$ denotes the complex conjugate quantity. $a > 0$ is the scale parameter, representing the dilation of mother function. \bar{b} is the shift parameter, representing the displacement of mother function. \mathbf{q} is the rotation angle and $r_{\mathbf{q}}$ is the rotation parameter which is defined as Eq. (3):

$$r_{\mathbf{q}} = \begin{bmatrix} \cos \mathbf{q} & \sin \mathbf{q} \\ -\sin \mathbf{q} & \cos \mathbf{q} \end{bmatrix} \quad (3)$$

The rotation parameter acts on \bar{x} as usual:

$$r_{\mathbf{q}} \bar{x} = (x \cos \mathbf{q} + y \sin \mathbf{q}, -x \sin \mathbf{q} + y \cos \mathbf{q}), \quad 0 \leq \mathbf{q} < 2\pi \quad (4)$$

The scale parameter a and the rotation parameter $r_{-\mathbf{q}}$ can be replaced by the new parameter A which is defined as Eq. (5):

$$A = ar_{-\mathbf{q}} \quad (5)$$

The wavelet function can be rewritten as Eq. (6):

$$\mathcal{Y}_{A, \bar{b}}(\bar{x}) = \frac{1}{|a|} \cdot \mathcal{Y} \left[A^{-1}(\bar{x} - \bar{b}) \right] \quad (6)$$

If the signal has a major component of the frequency corresponding to the given scale, then the wavelet at this scale is close to the signal at the particular location and the corresponding Wavelet transform coefficient, determined at this point, has a relatively large value. Therefore, the wavelet coefficients represent the correlation between the wavelet and a localized section of the signal.

Several mother wavelet functions $[\mathcal{Y}(x, y)]$ have been proposed in the literature, often designed for a specific problem. Given an image, without determination of directions, an isotropic wavelet will suffice, such as the radial Mexican hat wavelet. But, if directional features are to

be measured (segments, edges, vector field, ...), a directional or oriented wavelet function must be used. Because the wave pattern in an image is directional, the directional wavelet mother function should be chosen. The well-known Morlet wavelet function is thus adopted in this study. The 2-D Morlet wavelet function is:

$$\mathbf{y}(\bar{x}) = e^{i\bar{n}\cdot\bar{x}} \cdot e^{-\frac{1}{2}|\bar{n}|^2} \quad (7)$$

where \bar{n} is the oscillation parameter of the mother wavelet function. According to the functions of scale, rotation and shift parameters in the Wavelet transform, it is known that these parameters are related to the wavenumber (\bar{k}) of ocean waves and the representative position (\bar{x}) of image spectrum analysis respectively. The relations are derived in the following sections.

Due to the result of Wavelet transform result $S(a, \bar{b}, \mathbf{q})$ is a function of 4 variables: 2 position variables \bar{b} , and 2 frequency related variables (a, \mathbf{q}). One may say that the Wavelet transform has unfolded the signal from 2 to 4 dimensions. As a consequence, some of the variables must be fixed for visualization. The best way to interpret the outcomes of the Wavelet transform is to present the two-dimensional sections for the parameter space. They are

(1) the frequency representation: When the shift parameter \bar{b} is fixed, the WT outcome is considered as a function of frequency. The Wavelet spectrum can be obtained at different positions of the image are already known.

(2) the position representation: When the scale and rotation parameters (a, \mathbf{q}) are fixed, the WT outcome is considered as a function of position \bar{b} alone. The spatial energy distribution of specific component wave can be shown.

The position representation is useful for general purpose of image processing, such as detection of shape and contours of objectives, pattern recognition and image noise filtering. However, the frequency representation is particularly relevant to this study because it can be applied to the extraction of spectrum information for different positions in the non-homogeneous image.

Relationship between scale parameter (A) and wavenumber (\bar{k})

The frequency function $\hat{\mathbf{y}}$ is the Fourier transform of wavelet \mathbf{y} . The modulated $\hat{\mathbf{y}}$ by dilation, rotation and translation is written as Eq. (8).

$$\hat{\mathbf{y}}_{a, \mathbf{q}, \bar{b}}(\bar{k}) = a \cdot e^{-i\bar{b}\cdot\bar{k}} \cdot \hat{\mathbf{y}}(a\mathbf{r}_{-\mathbf{q}}(\bar{k})) \quad (8)$$

After the modulation, the gravity center of the wavelet function changes from the old gravity center (\bar{k}_g) to the new gravity center (\bar{k}_g^*).

$$\bar{k}_g^* = a\mathbf{r}_{-\mathbf{q}}\bar{k}_g \quad (9)$$

The scale and rotation parameter ($a\mathbf{r}_{-\mathbf{q}}$) is a matrix which can be replaced as the parameter A which is a mathematical matrix. The square value of wavelet function ($|\hat{\mathbf{y}}(\bar{k}_n)|^2$) is used as the weights. The new gravity center (\bar{k}_g^*) is then calculated by Eq. (10).

$$\bar{k}_g^* = \frac{(\bar{k}_1^*)|\mathbf{y}(\bar{k}_1^*)|^2 + (\bar{k}_2^*)|\mathbf{y}(\bar{k}_2^*)|^2 + \dots + (\bar{k}_n^*)|\mathbf{y}(\bar{k}_n^*)|^2}{|\mathbf{y}(\bar{k}_1^*)|^2 + |\mathbf{y}(\bar{k}_2^*)|^2 + \dots + |\mathbf{y}(\bar{k}_n^*)|^2} \quad (10)$$

where \bar{k}_i^* is the domain of modulated wavelet function $\hat{\mathbf{y}}$, and $\mathbf{y}(\bar{k}_i^*)$ is the corresponding value of $\hat{\mathbf{y}}$. The relationship between scale and rotation parameter (A) and wavenumber (\bar{k}) can be derived by transform of 2D wavelet function with a combination of Eq. (9) and Eq. (10) as shown in Eq. (11), which indicated scale parameter varies inversely with wavenumber. The smaller wavelength of component wave is, the larger is scale parameter will be in order to enlarge wavelet function to obtain enough wave information for analysis.

$$\bar{k} = A^{-1} \cdot \frac{\int_{-\infty}^{\infty} \bar{k}^* \cdot |\hat{\mathbf{y}}(\bar{k}^*)|^2 d\bar{k}^*}{\int_{-\infty}^{\infty} |\hat{\mathbf{y}}(\bar{k}^*)|^2 d\bar{k}^*} \quad (11)$$

VALIDATION OF PRESENTED IMAGE SPECTRUM ANALYSIS METHOD

In this section, the wave pattern images which include the homogeneous image of uni-directional regular wave, local non-homogeneous image of multi-directional regular wave and the non-homogeneous images are all simulated. The performance of 2D Wavelet spectrum analysis is assessed comparison with the results of Fourier transform.

Homogeneous Image of Uni-directional Regular Wave Pattern

The uni-directional regular wave is simulated by following equation.

$$I(x, y) = \sum_{i=1}^M a_i \cos[k_i(x \cos \mathbf{q}_i + y \sin \mathbf{q}_i)] \quad (12)$$

where \mathbf{q} is the wave direction of regular wave in the wave image. In this case, we let the parameter $M=1$. The wave coming from north is defined as zero degree and the angle increases clockwise. The regular wave image with 0.2 m wave height (a_i) and 10 m wavelength (k_i) and 45° wave direction (\mathbf{q}_i) is simulated as shown in Fig. 2.

It is found that the peak wavenumber of its Wavelet spectrum which is analyzed from location A equals to 0.62, meaning the wavelength is 10m and wave direction is found as 45°. They are the same values with the

input parameters of simulation. It is validated that the derived equation is right and the Wavelet transform has capability to analyze the homogeneous image. In addition, the result of Wavelet spectral analysis is found the same as Fourier spectral analysis due to the test image is homogeneous.

Local Non-homogeneous Image with Multi-directional Regular Wave Pattern

Image simulation

To verify the performance of wavelet transform in analyzing a non-homogeneous image, Eq. (14) with $M=4$ is used again to simulate a non-homogeneous image with the wave patterns of four different directions that are arranged in four quadrants respectively. The simulation conditions are listed in Table 1, and the simulated image is shown in Fig. 3 (Image II). The component waves in each quadrant are regular and homogeneous, while the margin of each quadrant and the whole image belong to non-homogeneity. Such an image is called as the local non-homogeneous image used to differentiate the image spectrum estimation by wavelet transform and Fourier transform.

Results

The image Fourier spectrum is obtained as shown in Fig. 4. The wavelengths of the four component waves located at wavenumber (k_x, k_y) equal to $(-0.68, 0.39)$, $(0.44, 0.44)$, $(0.54, 0.31)$ and $(0, -0.52)$ are 8m, 10m, 10m and 12m respectively and the corresponding wave directions are $-60^\circ, 45^\circ, 60^\circ$ and 180° that are match with input conditions. Although the energy density of Image II is presented in Fig. 4, yet in fact, the component wave with wavelength of 10 m and wave direction of 45° only exists in first quadrant not second instead; the component wave with wavelength of 8 m and wave direction of -60° only exist in second quadrant, etc. However, they are all presented in the unique Fourier spectrum without localization. This is not a reasonable solution.

When the Wavelet transform is applied, the spectral information in different position of the image is found due to its capability of extractable localization for local image characteristics. The Wavelet spectrum at location B in Fig. 3 is shown in Fig. 5. The deriving parameters are the same with the input parameters of the first quadrant of image II. When analyze the image spectrum at C that is located in position $\bar{b} = (105m, 95m)$, the widow size covers four quadrants, as shown in Fig. 3, there are four wave components as shown in Fig. 6. The spectral energy of the component waves appeared in Fig. 6 is proportion to the percentage of covered area of component waves in the location C. This validates the Wavelet transform is a correct method for extraction of image features even for the local non-homogeneous image.

Non-homogeneous Image with Random Wave Pattern

Image Simulation

In reality, the sea-state is extremely random and irregular. This section uses a random sea-state simulation method first presented by Goda & Mizusawa (1995) to simulate the near real sea-state image for testing the

developed image spectrum analysis method. The random wave field is represented by Eq. (14). The concept of directional wave spectrum is used to represent the amplitude of random waves a_i as shown in Eq. (13):

$$a_i = \sqrt{2 \cdot S(f, \mathbf{q}) \cdot Df \cdot Dq} \quad (13)$$

where $S(f, \mathbf{q})$ is the directional wave spectrum that is the product of frequency spectrum $S(f)$ and directional spreading function $D(f, \mathbf{q})$. Goda (1999) used the modified JONSWAP spectrum as the input of frequency spectrum. The simulated image is shown in Fig. 7 (Image III).

Results

Due to the outcome of Wavelet transform being a two-dimensional wavenumber spectrum. In order to compare with JONSWAP spectrum which we input. The spectral transform from wavenumber domain to direction-frequency spectrum at location D of Image III as shown in Fig. 8. The difference of wave direction between input spectrum and Wavelet spectrum is 2.7° and the differences of wavelength and peak frequency are 5.0m and 0.04Hz respectively. This test shows that the Wavelet transform could be used to extract spectrum features of the random sea-state.

Non-homogeneous Image Caused by Point Sources

Image simulation

In addition to regular and irregular wave field, there are some special wave patterns such as the waves produced from a source point. This wave pattern is similar to the tsunami wave caused by earthquake or the diffraction waves appeared near the breakwater. This wave pattern is called the "point-source wave field". These point-source waves are thought as non-homogeneity, at least on the wave direction property. The image of point-source wave field is simulated using Eq. (14). The wave pattern image caused by two point-sources is simulated in Fig. 9. Both of the wave heights are 1.0 m and wavelengths are 3.0m and 6.0m respectively for the component waves.

$$I(x, y) = \sin\left(\sqrt{x^2 + y^2}\right) \quad (14)$$

Results

The wavelength of component waves in the image of point-source wave field can be evaluated accurately by using Fourier transform as shown in Fig. 10. The peak energy occurred at the points whose wavelengths are 3 m and 6 m that are conformed to the given simulation conditions. However, the wave direction information obtained from Fourier transform is not from "point source", namely they scatter within a wide range that the waves do not come from the sources. In contrary, the accurate wavelength and wave direction information of where the component source waves come from by using wavelet transform is obtained as shown in Fig. 11. This case shows that the performance of application on non-homogeneous images by using Wavelet transform is

much higher than those using the Fourier transform.

ANALYSIS OF FIELD RADAR IMAGES

In this section, the presented method is used to test the field radar image for image spectrum analysis. Some institutes or research centers are developing the wave measurement technique by radar, such as the Coastal Ocean Monitoring Center of National Cheng Kung University in Taiwan and the German GKSS center (Ziemer and Dittmer, 1994). The marine radar image of Fig. 12 is provided by Prof. N.K. Liang of Institute of Oceanography of National Taiwan University. The water depth at the image place is about 20m. For the spectral analysis, the sub-image is always extracted out from the full radar image. The area of size 128×128 pixels is cut for image spectral analysis in this study. This sub-image is then transformed into image spectrum by applying the presented Wavelet approach. The resulting image spectrum is shown as Fig. 13. This case shows the capability of presented method on the image spectrum derivation of field radar images. More field radar images should be used for testing in the further study.

After the spectral analysis, the energy associated with the ocean waves could be separated from the background noise by applying the wave dispersion relation as a filter (Nieto et al., 1999). The noise energy is thus the difference between total energy and wave energy. The filtered spectral density obtained is related to the scale of the sampled gray levels. The calculation of the significant wave height for marine radar data is based on a similar technique as used for SAR system (Alpers & Hasselmann, 1982). After separating the wave signal from the background noise, the Signal to Noise Ratio (SNR) can be used to estimate the wave heights by the calibration with in-situ wave heights. This is the further processing of radar wave observation technique after the spectral analysis.

CONCLUSIONS

Wave remote sensing is an indirect observation method. Wave parameters are derived by image spectral analysis. In order to analyze the nearshore image, a non-homogeneous image spectrum analysis method is developed in this study. This method is developed based on Wavelet transform. The homogeneous and non-homogeneous images are simulated to test the performance of spectral analysis of presented method by comparing with traditional Fourier method. It is validated that the presented method has higher capability on localization of local spectrum property than Fourier method, especially for the nearshore non-homogenous images. In addition to the simulated images, the field X-band marine radar images are analyzed. It is found that the image spectrum can be successfully estimated, verifying the potential of the presented method for image spectral analysis.

ACKNOWLEDGEMENTS

This study is supported by National Science Council (NSC) of Taiwan, Republic of China under the project number NSC 91-2611-E-006-013. Prof. N. K. Liang in the Institute of Oceanography of National Taiwan University provided the radar images for this study. The authors would like to show the great thanks here.

REFERENCES

- Alpers, W., Hasselmann, K. (1982). "Spectral signal to clutter and thermal noise properties of ocean wave imaging synthetic aperture radars," *International Journal Remote Sensing*, Vol 3, pp 423–446.
- Bendat, J.S., Piersol, A.G. (1986). "Random Data: Analysis and Measurement Procedures," John Wiley and Sons, New York, Chichester, Brisbane, Toronto and Singapore.
- Chui C.K., Montefusco L., Puccio L. (1994). "Wavelets: Theory, Algorithms and Applications," Academic Press, Boston.
- Daubechies, Ingrid (1990). "Wavelet transform, time-frequency localization and signal analysis," *IEEE Transactions on Information Theory*, Vol. 36, No. 5, pp 961-1005.
- Doong, DongJiing, Wu, Lee Chung, Kao, Chia-Chuen, Chuang, Z. H. Laurence (2001). "Wave Spectra Derived by CWT on the Radar Images," *International Conference on Port and Maritime R&D and Technology*, Singapore.
- Goda, Y. and Mizusawa, T. (1995). "Spatial and temporal fluctuations of nearshore currents induced by directional random waves," *Proc. Coastal Dynamics '95*, pp 269-280, ASCE.
- Goda (1999). "A comparative review on the functional forms of directional wave spectrum," *Coastal Eng. J.*, Vol. 41(1), 1-20.
- Hasselmann, K., R. K. Raney, W. J. Plant, W. Alpers, R. A. Shuchman, D. R. Lyzenga, C. L. Rufenach, and M. J. Tucker (1985). "Theory of synthetic aperture radar ocean imaging: A MARSEN view," *Journal of Geophysics Research*, Vol 90, pp 4659-4686.
- Kuo, Y. Y., L. G. Leu and I. L. Kao (1999). "Directional spectrum analysis and statistics obtained from ERS-1 SAR wave images," *Ocean Engineering*, Vol 26, pp 1125-1144.
- Massel, S.R. (2001). "Wavelet analysis of processing ocean surface wave records," *Ocean Engineering*, Vol 28, pp 957-987.
- Nieto Borge, J.C., Hessner, K., Reichert, K. (1999). "Estimation of the Significant Wave Height with X-Band Nautical Radars," *OMAE 1999*.
- Nieto Borge, J.C., Reichert, K., Dittmer, J. (1999). "Use of nautical radar as a wave monitoring instrument," *Coastal Engineering*, Vol 37, pp 331–342.
- Nieto Borge, J. C., Konstanze Reichert and Jurgen Dittmer (1999). "Use of nautical radar as a wave monitoring instrument," *Coastal Engineering*, Vol 37, pp 331–342.
- Seemann J., C.M. Senet, F. Ziemer (1997). "A method for computing calibrated ocean wave spectra from measurements with a nautical X-Band radar," *Proceedings of OCEAN'97*, Halifax, Canada.
- Ziemer, F. and J. Dittmer (1994). "A system to monitor ocean wave fields," *Proceedings of the OCEANS'94*, Vol. II, pp. 28 - 31.

Table 1 Simulation conditions of local non-homogeneous image

| No. of component waves | Location of component waves | Wave height (m) | Wavelength (m) | Wave direction (degree) |
|------------------------|-----------------------------|-----------------|----------------|-------------------------|
|------------------------|-----------------------------|-----------------|----------------|-------------------------|

| | | | | |
|-----|-----------------|------|----|-----|
| (1) | First quadrant | 0.20 | 10 | 45 |
| (2) | Second quadrant | 0.15 | 8 | -60 |
| (3) | Third quadrant | 0.25 | 10 | 60 |
| (4) | Forth quadrant | 0.10 | 12 | 180 |

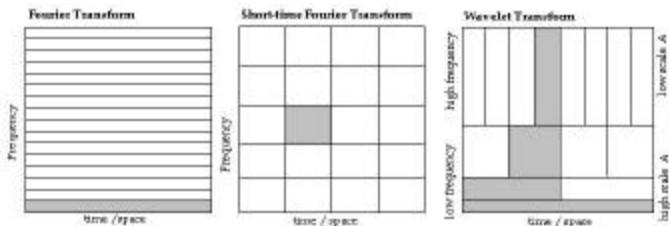


Fig. 1 The time/space-frequency resolution scheme of FT, STFT and WT

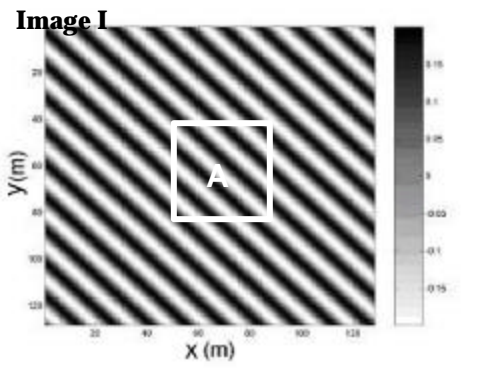


Fig. 2 Simulation images I (homogeneous) with uni-directional regular wave pattern

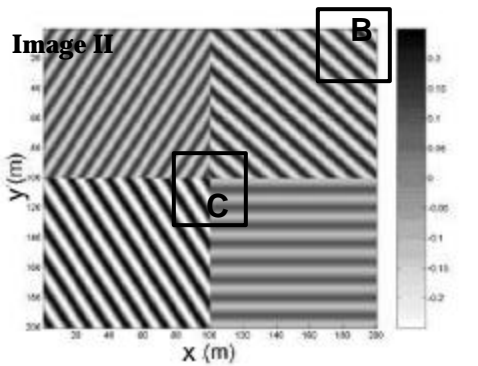


Fig. 3 Simulation Image II (local non-homogeneous) with multi-directional regular wave pattern

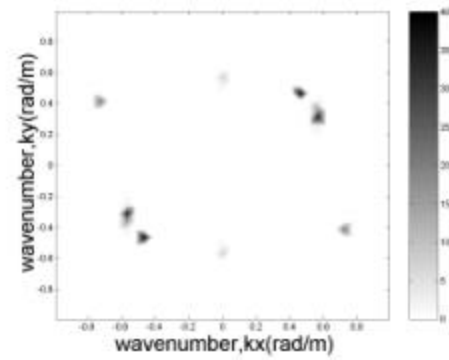


Fig. 4 Fourier spectrum of image II

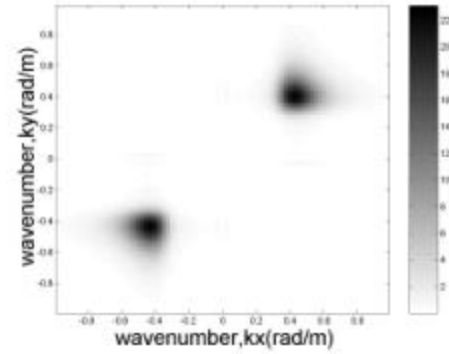


Fig. 5 Wavelet spectrum at B of Image II

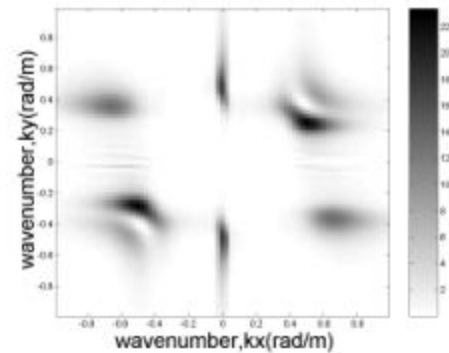


Fig. 6 Wavelet spectrum at C of Image II

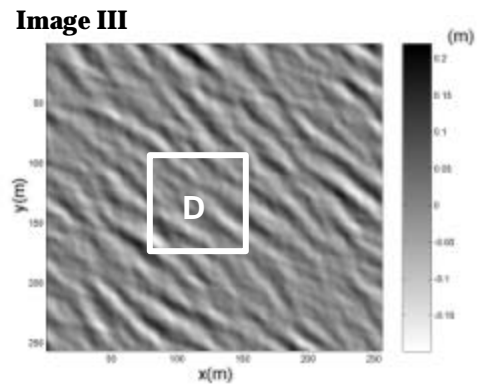


Fig. 7 Simulation Image III (non-homogeneous)

with random wave pattern

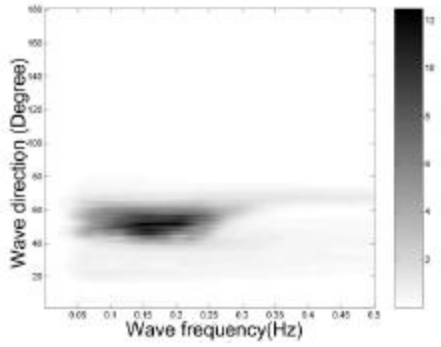


Fig. 8 Directional Wavelet spectrum at D of Image III

Fig. 10 Fourier spectrum of image IV

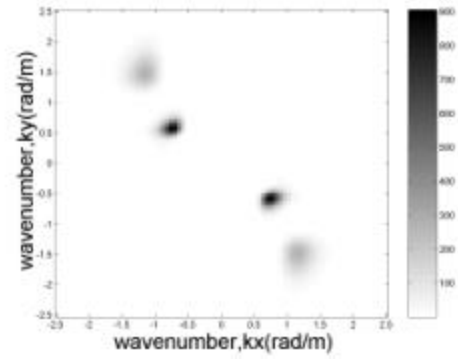


Fig. 11 Wavelet spectrum at E of Image IV

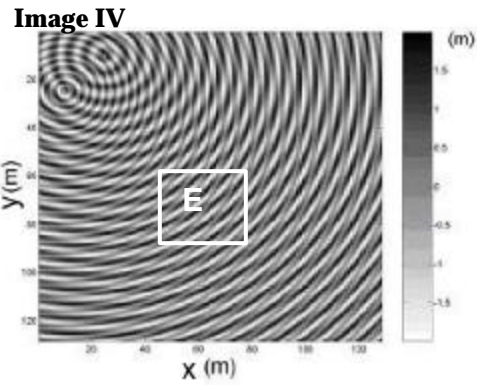


Fig. 9 Simulation Image IV (non-homogeneous) with wave pattern coming from two source-points

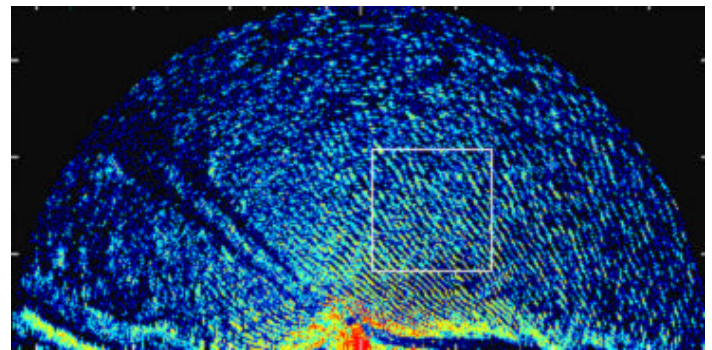


Fig. 12 The field marine radar image

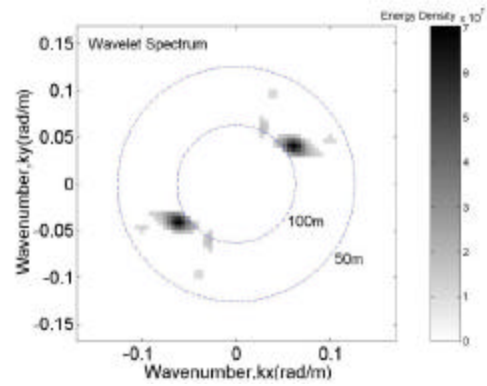
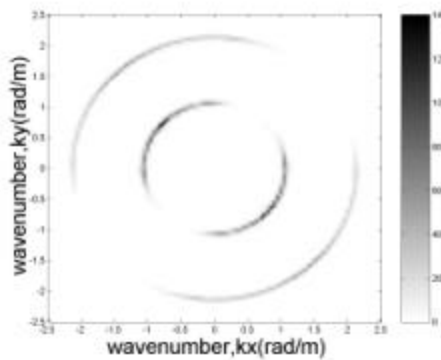


Fig. 13 Wavelet spectrum of the field marine radar image